

# Contribution of the nucleon-hyperon reaction channels to $K^-$ production in proton-nucleus collisions

H.W. Barz and L. Naumann

Forschungszentrum Rossendorf, Pf 510119, 01314 Dresden, Germany

## Abstract:

The cross section for producing  $K^-$  mesons in nucleon-hyperon collisions is estimated using the experimentally known pion-hyperon cross sections. The results are implemented in a transport model which is applied to calculation of proton-nucleus collisions. Contrarily to earlier estimates in heavy-ion collisions the inclusion of the nucleon-hyperon cross section roughly doubles the  $K^-$  production in near-threshold proton-nucleus collisions.

PACS numbers: 25.40.-h, 25.70.-q

Keywords:  $K^-$  meson production, proton-nucleus collisions

## 1 Introduction

The properties of strange mesons within nuclear matter has been subject to numerous investigations. Especially nuclear collisions at energies near or below the production threshold of nucleon-nucleon collisions should be very sensitive to the kaon properties in matter [1]. Early theoretical approaches based on effective chiral Lagrangians [2] predicted an attractive scalar potential which together with an isovector potential leads to a strong attractive  $K^-$  and a moderately repulsive  $K^+$  potential. These potentials depend only weakly on the momentum. Indeed kaonic atoms require a strong attractive  $K^-$  potential and also the large  $K^-$  rates observed in heavy-ion collisions, carried out by the FOPI [3, 4] and KaoS [5, 6, 7, 8, 9] collaborations, seemed to support these predictions. However, more sophisticated theoretical investigations [10, 11, 12] demonstrated a strong momentum dependence of the

potentials which even became repulsive at large density and momentum for both  $K^+$  and  $K^-$  mesons. These potentials do not comply with the early analyses of the measurements of  $K^-$  production. However one has to keep in mind that the elementary cross sections for  $K^-$  production used are not very well known from experiment.

The knowledge of the production mechanism of kaons is a necessary condition to probe the theoretical predictions for the potentials. In this respect it is useful to study also nucleon-nucleus collisions as a further source of information.

In nucleus-nucleus collision antikaons have been observed at ion bombarding energy of 1.5 GeV per nucleon [5, 6, 7, 8, 9, 13, 14]. This energy is far below the threshold energy of 2.5 GeV for nucleon-nucleon collisions. This nucleon-nucleon production channel is unimportant in heavy-ion collisions due to the smallness of the kaon pair production cross section [15] even if Fermi motion would help to overcome the threshold. The antikaons can however be produced by multistep-scattering processes. In the sequence of the collisions combined with Fermi motion strangeness transfer via  $\pi Y \rightarrow NK^-$  reactions can take place with their comparably large cross sections.

Only a few data for antikaon production in nucleon-nucleus collision near threshold are available. We compare our calculations with the KaoS data [16]. A comparison to additional existing antikaon data from FHS [17] below and KEK-PS [18] above threshold seems not to be reasonable, because of their very strong kinematical constraint. In nucleon-nucleus collisions the above mentioned  $\pi Y$  channel is a rather improbable three step process, because the single incoming proton alone has to produce both reaction partners before. Also the second chance collision  $\pi N \rightarrow NK^+K^-$  channel has the small cross section of the kaon pair production. Therefore, in a second chance collision the antikaon could mainly be produced via the  $NY \rightarrow NNK^-$  channel which is open for an incident proton energy larger than 1.73 GeV. Additional Fermi motion may lead to a further reduction of the threshold.

Therefore we draw our attention to the nucleon-hyperon channel  $NY \rightarrow NNK^-$  cross section. This cross section was already calculated early in the one-pion exchange model [19] and later in one-boson exchange approximation [20, 21] and was found to be unimportant for heavy-ion collisions. Here we reevaluate the cross section within a different approach avoiding the uncertainties arising from the badly known formfactors when applying an effective perturbation theory. Our results roughly agree with the cross sections obtained in ref. [20, 22]. In the relevant kinetic energy region the cross section reaches nearly one mb and is about 50 times larger than the related cross

sections of the reactions  $NN \rightarrow NYK^+$ . As the ratio of hyperons as well as of kaons to the participating nucleons is about  $10^{-4}$  this would lead to a  $K^-$  to  $K^+$  ratio of about  $10^{-2}$  which is nearly the magnitude of the measured ratio at 2.5 GeV beam energy. Thus, this channel should compete with the NN and  $\pi Y$  production channels.

In addition we mention that the in-medium cross sections may considerably differ from their vacuum values. This was pointed out e.g. in ref. [11] where a considerable enhancement of the pion-hyperon channels have been predicted. These results are based on coupled channel calculations and are connected with a shift of the masses of the  $\Lambda(1405)$  and  $\Sigma(1385)$  resonances in nuclear matter. This effect will not be considered here.

## 2 Elementary cross sections

To estimate the  $NY \rightarrow NNK^-$  cross sections we start with the Feynman diagrams shown in Fig. 1 which are similar for  $NY \rightarrow NNK^-$  and  $NN \rightarrow NYK^+$  processes. The  $K^\pm$  mesons are generated by the subprocess where the intermediate meson (here a pion) interacts with the second baryon. This subprocess cannot be calculated for certainty because many resonances contribute with unknown coupling constants. The results of such one-boson exchange reactions can be found in ref. [20]. Here we will approach the study of these cross sections differently by making the assumption that the most important meson exchange is that of a pion. The  $\pi B \rightarrow K^\pm$  cross sections are known experimentally from which we can extract the square of the transition matrix elements  $T_{\pi B}$  illustrated by the hatched areas in Fig. 1. Then, these values are used to calculate the cross sections in accordance with the diagram in Fig. 1. We calculate both the kaon and the antikaon production in order to check the method since the cross sections for  $NN \rightarrow NYK^+$  [23] has been calculated and adjusted to the partially known pp cross sections [24].

Thus we consider the process  $N_1+B_2 \rightarrow N_3+B_4 + K(\bar{K})$ , where the symbol N denotes a nucleon with isospin  $I_1 = I_3 = 1/2$  and one of the symbols  $B_2$  or  $B_4$  stands for a hyperon. The pion-nucleon coupling in the left hand vertex in Fig. 1 is described by the lagrangian

$$\mathcal{L}_{\pi NN} = g\bar{\psi}\gamma^5\vec{\tau}\psi\vec{\pi} \quad (1)$$

with  $\psi$  denoting the nucleon field,  $\vec{\pi}$  the pion field,  $\vec{\tau}$  the isospin Pauli matrix,  $\gamma^5$  is a Dirac matrix, and  $g = 13.6$  fixes the pion-nucleon coupling constant. The spin and isospin averaged cross section for the process at the center-of-

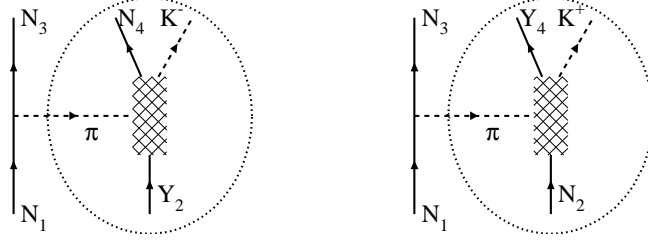


**Figure 1:** Diagram for antikaon (left) and kaon (right) production in the process  $N+Y(N) \rightarrow N+N(Y)+K^- (K^+)$  by pion exchange. The  $T$  matrix describing processes within the hatched box is determined from experimental data.

mass energy  $\sqrt{s}$  reads

$$\begin{aligned}
\sigma_K &= \frac{g^2}{2\lambda^{1/2}(m_1^2, m_2^2, s)} \frac{1}{(2\pi)^5} \frac{1}{8(2I_2 + 1)} \\
&\times \sum_{spin, isospin} |\langle I_3 | \vec{\tau} | I_1 \rangle|^2 \int d^4 p_\pi \frac{d^3 \mathbf{p}_4}{2p_4^0} \frac{d^3 \mathbf{p}_K}{2p_K^0} |(\bar{u}_3 \gamma^5 u_1)|^2 \\
&\times \delta((p_1 - p_\pi)^2 - m_3^2) \delta^4(p_\pi + p_2 - p_3 - p_K) \left| \frac{1}{p_\pi^2 - m_\pi^2} T_{\pi B_2: B_4 K} \right|^2,
\end{aligned} \quad (2)$$

where the indices of the momenta  $p$  and masses  $m$  are those used in Fig. 1,  $u$  denotes the nucleon spinor, and  $\lambda(a, b, c) = (s - a - b)^2 - (2ab)^2$  is the triangle function, and  $I_2$  stands for the isospin of particle  $B_2$ . The integral over the outgoing momentum  $p_3$  of particle  $N_3$  has been substituted by the pion momentum  $p_\pi = p_1 - p_3$ . The symbol  $T_{\pi B_2: B_4 K}$  represents the encircled part in Fig. 1 which determines the kaon (antikaon) production in pion-baryon collisions the cross section of which is given by

$$\begin{aligned}
\sigma_{\pi B_2} &= \frac{1}{2\lambda^{1/2}(m_\pi^2, m_2^2, s_{\pi B_2})} \frac{1}{(2\pi)^2} \frac{1}{6(2I_2 + 1)} \\
&\times \sum_{spin, isospin} \int \frac{d^3 \mathbf{p}_4}{2p_4^0} \frac{d^3 \mathbf{p}_K}{2p_K^0} \delta^4(p_\pi + p_2 - p_3 - p_K) |T_{\pi B_2: B_4 K}|^2.
\end{aligned} \quad (3)$$

This cross section depends on the square of the center-of-mass energy  $s_{\pi B_2} = (p_\pi + p_2)^2$  with the on-shell condition  $p_\pi^0 = \sqrt{m_\pi^2 + \mathbf{p}_\pi^2}$ . Notice that in Eq.(2) the pion momentum  $p_\pi$  is off-shell.

Inserting Eq.(3) into Eq.(2), summing over the spin quantum numbers

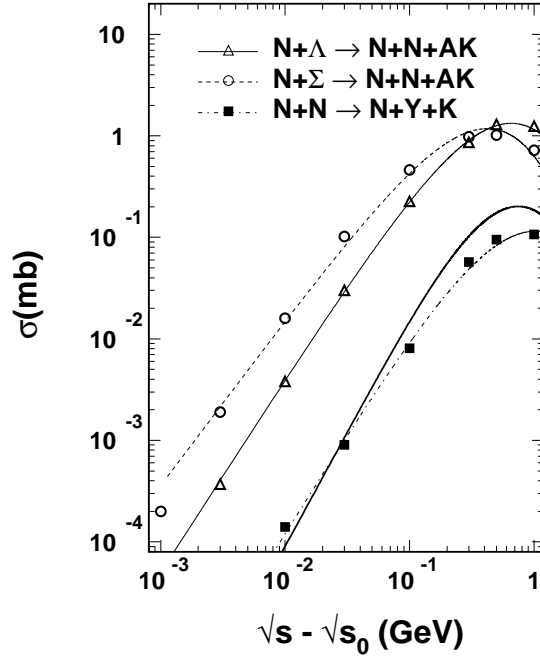


**Figure 2:** Isospin averaged production cross sections for kaon (full squares) and antikaon (open symbols) production versus excess energy. The thin lines are parametrizations (described in text) adjusted to the calculated values (symbols) whereas the thick line displays the cross section for  $K^+$  production as calculated in ref. [23].

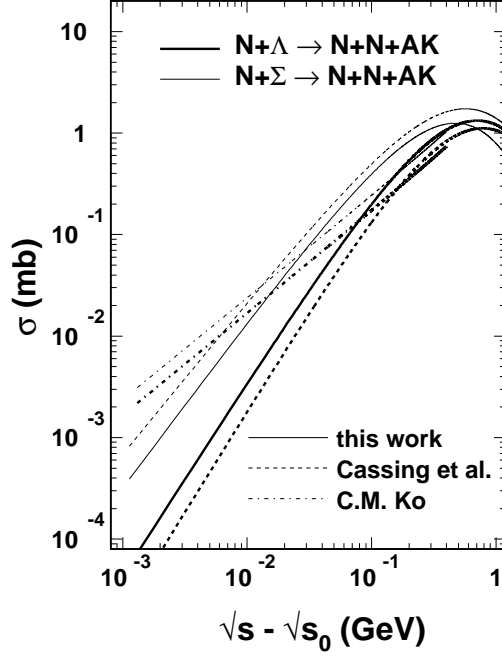


**Figure 3:** Comparison of isospin averaged production cross sections for antikaon production versus excess energy obtained by various models. The thick (thin) curves describe the  $N\Lambda$  ( $N\Sigma$ ) collisions. The full lines depict our results, the dot-dashed and dashed lines are results from [19] and [22], respectively.

of the nucleons and integrating out the time component  $p_\pi^0$  of the pion momentum we obtain the cross section

$$\begin{aligned} \sigma_K &= \frac{g^2}{\lambda^{1/2}(m_1^2, m_2^2, s)} \frac{1}{(2\pi)^3} \int \frac{d^3\mathbf{p}_\pi}{\sqrt{m_3^2 + \mathbf{p}_\pi^2}} \frac{p_1 \cdot p_3 - m_1 m_3}{(p_\pi^2 - m_\pi^2)^2} \\ &\times f^4(p_\pi) \lambda^{1/2}(m_\pi^2, m_2^2, s_{\pi B_2}) \sum_{I_\pi} \sigma_{\pi B_2}(s_{\pi B_2}), \end{aligned} \quad (4)$$

where the formfactor

$$f(p_\pi) = \frac{\Lambda^2 - m_\pi^2}{\Lambda^2 - p_\pi^2} \quad (5)$$

with  $\Lambda = 1.6$  GeV [25] has been introduced.

The cross sections  $\sigma_{\pi B_2}$  needed in Eq.(4) for the reactions  $\pi Y \rightarrow NK^-$  can be derived from the measured inverse reactions  $K^- p \rightarrow \Sigma^+ \pi^-$ ,  $\Lambda \pi^0$ ,  $\Sigma^- \pi^+$  and  $K^- n \rightarrow \Lambda \pi^-$ ,  $\Sigma^- \pi^0$  which are given in ref. [24]. The  $K^0 N$  cross sections are derived by isospin reflection.

The results for the antikaon production in  $N\Sigma$  and  $NA$  collisions are represented by the open symbols in Fig. 2. The lines through the symbols show fits with the standard parametrization  $\sigma \propto (s - s_0)^a/s^b$ . The  $K^+$  cross section is compared to the parametrization of ref. [23] which gives in the low energy region nearly the same cross section but underestimates the cross section above 100 MeV. The parametrization in ref. [23] is based on a model which uses diagrams which have the same structure as those of Fig. 1. In that investigation an exchange of  $\pi$ ,  $\eta$  or  $\rho$  mesons is included, and it is shown that the pion gives the main contribution, a fact that supports our assumption of the dominance of the pion exchange.

In Fig. 3 we compare the curves in Fig. 2 to the results of previous calculations [19, 20, 22]. There are only small deviations from the calculations in the one-boson exchange approximation [20, 22] which also shows the dominance of the  $N\Sigma$  channel. The result [19] has a weaker energy dependence but provides comparable cross section in the relevant energy region of about 100 MeV above threshold. In this investigation it was also shown that this channel could contribute about 10% to the  $K^-$  production in heavy-ion collisions. In our following calculations we find that even half of the antikaons can stem from the  $NY$  channel in proton-nucleus collisions.

### 3 Comparison to data

It is our aim to study the role of the  $NY \rightarrow NNK^-$  reaction in pA collisions. Usually these channels are not included in standard analyses of those reactions which consider only the elementary  $BB$  and  $\pi B$  collisions. To study this question we additionally incorporate the  $NY$  channels into a transport model calculation which is based on the Boltzmann-Ühling-Uhlenbeck equation [27]. Furthermore, the production rate of the  $K^-$  mesons also depends sensitively on the attractive  $K^-$  potential. Therefore, the inclusion of different production channels will effect predictions on the size of this potential when derived from comparison with data.

In Fig. 4 we present the differential cross sections at a laboratory angle of  $40^\circ$  for collisions of protons with  $^{12}\text{C}$  and  $^{197}\text{Au}$  at 2.5 GeV beam energy. The dotted lines are calculated without using potentials for the kaons and antikaons. These calculations underestimate clearly the measured data [16]. The attractive antikaon potential,

$$V_{\bar{K}} = -0.08 \text{ GeV} \frac{n}{n_0} \quad (6)$$

in addition with the  $NY$  channels leads to an increase of the cross section

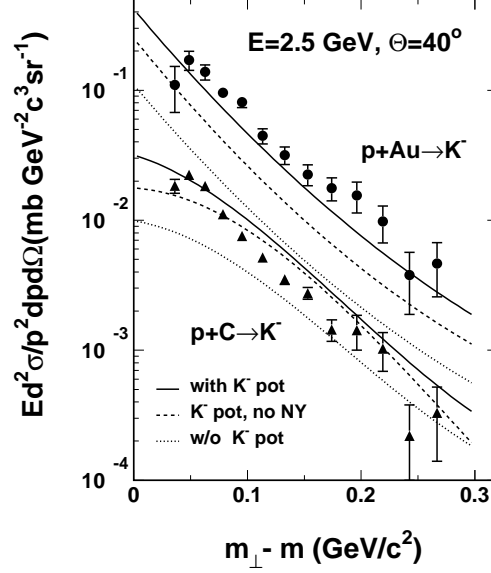


**Figure 4:** Comparison of measured [16] invariant  $K^-$  meson cross sections (symbols) as a function of the transverse mass with calculations for proton collisions on C and Au targets at 2.5 GeV beam energy. The full (dotted) lines are calculated with (without) an antikaon potential while the dashed curves are obtained without the contribution of the nucleon-hyperon channel.

as shown by the full lines. Such a potential improves the agreement with the data. The dashed curves are results where the  $NY \rightarrow K^-$  channels has been excluded. Disregarding these channels the cross section diminishes by about 50% in p+Au collisions. This shows the importance of the  $NY \rightarrow K^-$  channels when one intends to determine the  $K^-$  potential. For the light C target the influence is much smaller as the hyperons have a smaller chance to collide with further nucleons before leaving the reaction zone.

Finally, we compare in Fig. 5 our calculations for  $K^+$  and  $K^-$  production with data obtained by the KaoS collaboration [16] for proton-nucleus collisions at bombarding energies of 2.5 GeV and 3.5 GeV on C and Au targets and K meson emission angles of  $40^\circ$  and  $56^\circ$ . The kinetic beam energy  $T_{\text{kin}} = 2.5$  GeV was close to the production threshold in nucleon-nucleon collisions. In the calculations we have used the parametrizations of ref. [23, 26]

and obtained kaon cross sections which are slightly smaller than the data for the gold target for both angles.

The kaon and antikaon production yields are related in the threshold region since nearly all of the antikaons are created in collisions of pions and nucleons with hyperons, the number of which equals to the kaon number because of strangeness conservation. This fact also holds if a chemical equilibrium between  $K^-$  and  $Y$  is reached via the  $K^-N \leftrightarrow \pi Y$  reaction [28, 30]. Therefore it is interesting to compare the ratio of the angle integrated cross sections for  $K^-$  to those of  $K^+$ . In Tab. 1 we display the calculated values and the experimental results obtained within the measured phase space by the KaoS collaboration [16]. Our calculations overestimate this ratio for 2.5 GeV but underestimate it for the higher energy of 3.5 GeV.

**Tab. 1** Comparison of calculated and experimentally obtained antikaon to kaon cross-section ratios for proton collisions on carbon  $R(C)$  and gold  $R(Au)$ . Experimental values with errors of about 20% are taken from [16].

$T_{kin}(\text{GeV})$	$R_{exp}(C)$	$R_{calc}(C)$	$R_{exp}(Au)$	$R_{calc}(Au)$
2.5	0.0085	0.013	0.0074	0.010
3.5	0.028	0.024	0.027	0.024

## 4 Conclusions

We have calculated the cross sections of antikaon-production in near-threshold proton collisions on carbon and gold targets. Comparison of our calculations with both kaon and antikaon data from the KaoS collaboration [16] were made at beam energies of 2.5 and 3.5 GeV for laboratory angles of  $40^\circ$  and  $56^\circ$ . Including the  $NY \rightarrow NNK^-$  channels nearly doubles the antikaon yield for collisions of protons on heavy targets like Au. No significant influence was found for the light carbon target. Calculated ratios of  $K^-$  to  $K^+$  cross sections came also reasonably close to the data. We conclude that the  $NY \rightarrow NNK^-$  channels have to be included in realistic calculations, especially for heavy targets, in order to study the properties of strange mesons in nuclear matter at normal nuclear density.

## Acknowledgments

Valuable discussions with Werner Scheinast and Burkhard Kämpfer are acknowledged. We thank Christoph Hartnack for informing us on similar results in his study. This work was supported in part by the BMBF grant

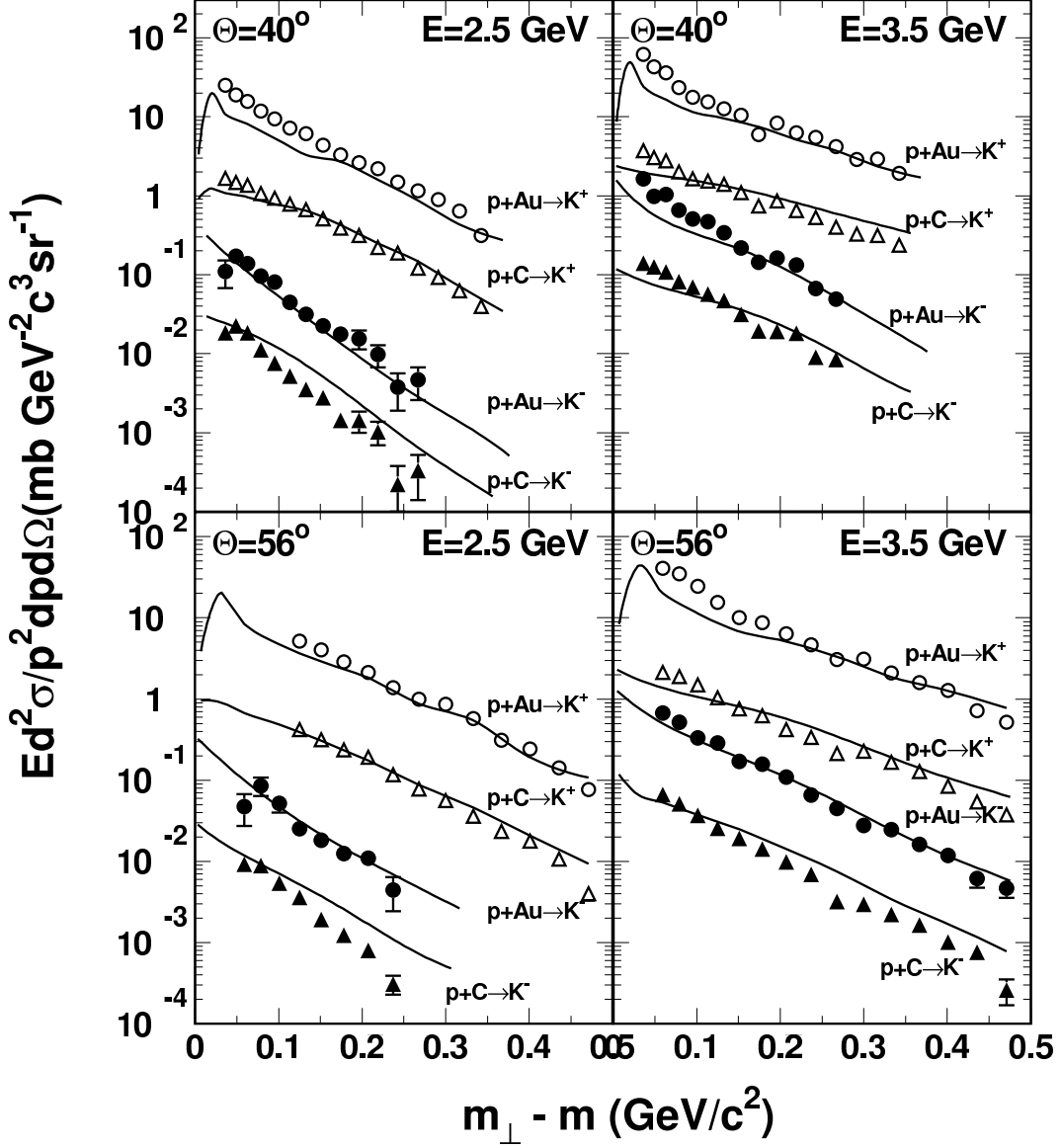


**Figure 5:** Invariant differential  $K^\pm$  cross section versus  $K$ -meson transverse mass at 2.5 and 3.5 GeV proton beam energy. The solid lines refer to our calculations including the NY channels for the antikaon production. Data are taken from ref. [16].

06DR121.

## References

- [1] J. Aichelin and C.M. Ko, Phys. Rev. Lett. **55** (1985) 2661
- [2] D.B. Nelson and A.E. Kaplan, Phys. Lett. **B 175** (1986) 57
- [3] N. Herrmann et al. (FOPI collaboration), Nucl. Phys. **A 610** (1996) 49c
- [4] K. Wisniewski et al. (FOPI collaboration), Eur. Phys. J. A **9** (2000) 515
- [5] R. Barth et al. (KaoS collaboration), Phys. Rev. Lett. **78** (1997) 4007
- [6] F. Laue et al. (KaoS collaboration), Phys. Rev. Lett. **82** (1999) 1640
- [7] F. Laue et al. (KaoS collaboration), Eur. Phys. Journal A **9** (2000) 397
- [8] M. Menzel et al. (KaoS collaboration), Phys. Lett. **B 495** (2000) 26
- [9] A. Förster et al. (KaoS collaboration), submitted to Phys. Rev. Lett.
- [10] A. Sibirtsev and W. Cassing, Nucl. Phys. **A 641** (1998) 476
- [11] J. Schaffner-Bielich, V. Koch, and M. Effenberger, Nucl. Phys. **A 669** (2000) 153
- [12] M.F.M. Lutz, E.E. Kolomeitsev, Nucl. Phys. **A 700** (2002) 193
- [13] A. Shor et al., Phys. Rev. Lett. **63** (1989) 2192
- [14] A. Schröter et al., Z. Phys. **A 350** (1994) 101
- [15] C. Quentmeier et al. (COSY-11 collaboration), Phys. Lett. **B 515** (2001) 276
- [16] W. Scheinast (KaoS collaboration), Meson 2002, World Scientific Publ. (Singapore) 2003, p. 493, ISBN 981-238-160-0
- [17] A. V. Akhmedov et al., Preprint ITEP 41-99 (1999)
- [18] Y. Sugaya et al., Nucl. Phys. **A 634** (1998) 115
- [19] C. M. Ko, Phys. Rev. C **29** (1984) 2169
- [20] W. Cassing, E.L. Bratkovskaya, U. Mosel, S. Teis, and A. Sibirtsev, Nucl. Phys. **A 614** (1997) 415
- [21] W. Cassing and E.L. Bratkovskaya, Phys. Rep. **308** (1999) 65
- [22] W. Cassing, private communication

- [23] K. Tsushima, A. Sibirtsev, A.W. Thomas, and G.Q. Li, Phys. Rev. C **59** (1999) 369, Erratum C **61** (2000) 029903
- [24] A. Baldini, V. Flaminio, W.G. Moorhead, and D.R.O. Morrison, Landolt-Börnstein, Band 12, Springer, Berlin 1988
- [25] R. Machleidt, Adv. Nucl. Phys. **19** (1989) 189
- [26] K. Tsushima, S.W. Huang, and A. Faessler, Austral. J. Phys. **50** (1997) 35
- [27] Gy. Wolf, W. Cassing, and U. Mosel, Nucl. Phys. **A 552** (1993) 549
- [28] G.Q. Li and G.E. Brown, Phys. Rev. C **58** (1998) 1698
- [29] T. Waas, N. Kaiser, and W. Weise, Phys. Lett. **B 379** (1996) 34
- [30] Ch. Hartnack, H. Oeschler, and J. Aichelin, Phys. Rev. Lett. **90** (2003) 102302